



## Engineering the thermostability of a TIM-barrel enzyme by rational family shuffling

Szilárd Kamondi, András Szilágyi, László Barna, Péter Závodszyk\*

Institute of Enzymology, Biological Research Center, Hungarian Academy of Sciences, Pf. 7, H-1518 Budapest, Hungary

### ARTICLE INFO

#### Article history:

Received 18 July 2008

Available online 27 July 2008

#### Keywords:

Thermal stability  
Rational family shuffling  
( $\beta/\alpha$ )<sub>8</sub>-Barrel fold  
Xylanase  
Chimera  
*Thermotoga maritima*

### ABSTRACT

A possible approach to generate enzymes with an engineered temperature optimum is to create chimeras of homologous enzymes with different temperature optima. We tested this approach using two family-10 xylanases from *Thermotoga maritima*: the thermophilic xylanase A catalytic domain (TmxAcat,  $T_{opt} = 68$  °C), and the hyperthermophilic xylanase B (TmxB,  $T_{opt} = 102$  °C). Twenty-one different chimeric constructs were created by mimicking family shuffling in a rational manner. The measured temperature optima of the 16 enzymatically active chimeras do not monotonically increase with the percentage of residues coming from TmxB. Only four chimeras had a higher temperature optimum than TmxAcat, the most stable variant ( $T_{opt} = 80$  °C) being the one in which both terminal segments came from TmxB. Further analysis suggests that the interaction between the N- and C-terminal segments has a disproportionately high contribution to the overall thermostability. The results may be generalizable to other enzymes where the N- and C-termini are in contact.

© 2008 Elsevier Inc. All rights reserved.

Microorganisms occur in almost all environments on Earth, including high-temperature environments such as hot springs. In most cases, proteins from (hyper)thermophilic organisms have been found to be structurally similar to their mesophilic counterparts, except for minor differences [1–3]. Recent studies have shown that compactness, contact order, and the density of salt bridges may be the primary factors that result in enhanced thermal stability of proteins [4–6].

The ( $\beta/\alpha$ )<sub>8</sub>-barrel fold, which was found in triose-phosphate isomerase, and is therefore also known as the TIM-barrel fold, is the most common enzyme fold [7]. ( $\beta/\alpha$ )<sub>8</sub>-barrel enzymes cover five of the six enzyme classes defined by the Enzyme Commission, acting as oxidoreductases, transferases, lyases, hydrolases and isomerases [7]. Overall, hydrolases (especially glycosidases) are the dominating class, comprising about half of the known ( $\beta/\alpha$ )<sub>8</sub>-barrels [7]. Structure-thermostability relationships and the engineering of glycoside hydrolases have attracted considerable current interest [8–10]. Family-10 xylanases perform glycosidic-bond hydrolysis with net retention of anomeric configuration via the double displacement mechanism involving two glutamate residues [11–13]. Hydrolysis of the  $\beta$ -1,4-glycosidic bonds of xylan, the major constituent of hemicellulose in the plant cell wall, is important in the paper, food and animal feed industries. When xylanases are used in biotechnological processes operating at elevated temperatures, a high thermal stability of the enzyme is a

desirable property because it reduces costs by extending the life of the biocatalyst. Ideally, the optimum working temperature of the enzyme should be the temperature where the biotechnological process operates, also considering the thermal stabilities of the other components.

In the present study, we used two family-10 xylanases from the hyperthermophilic eubacterium *Thermotoga maritima* MSB8 with widely different temperature optima as starting points for rational family shuffling [14] to construct chimeric enzymes with various optimum working temperatures in the thermophilic temperature range, in order to test this approach and to find the key stabilizing regions of the protein. Xylanase B (TmxB) is a hyperthermophilic enzyme with an optimum working temperature  $T_{opt} = 102$  °C, while the catalytic domain of xylanase A (TmxAcat) is thermophilic with  $T_{opt} = 68$  °C. TmxB is a well characterized enzyme with a known three-dimensional structure [5,15,16]. TmxAcat, the middle domain in a five-domain chain, has been cloned with various N- and C-terminal boundaries by Winterhalter et al. [17]. Twenty-one chimeras were constructed and several of them were found to have a higher thermal stability than TmxAcat, and it was found that the two terminal segments have a disproportionately large contribution to thermal stability.

### Materials and methods

*Construction of chimeric enzymes.* Genes *xynAcat* (GenBank Accession No. Z46264, basepairs 1340–2323) and *xynB* (GenBank Accession No. AAD35164) encoding TmxB and TmxAcat were PCR

\* Corresponding author. Fax: +36 1 4665465.

E-mail address: [zxp@enzim.hu](mailto:zxp@enzim.hu) (P. Závodszyk).

amplified from the genomic DNA of *T. maritima* MSB8, which was provided by Robert Huber (Universität Regensburg, Germany).

Chimeric enzymes were constructed by shuffling segments of the nucleotide sequences of the parental genes using a self-priming PCR reaction. Five highly similar regions suitable as shuffling sites were identified in a nucleotide sequence alignment prepared by the SIM algorithm (<http://expasy.ch/tools/sim.html>) [18] (see Fig. S1 in the Supplementary Material). To select suitable sites, the similarity of the two aligned sequences was checked in a 19-basepair window sliding along the alignment. The criterion for selection was that the number of differing nucleotides within the window must be less than three, and the differing nucleotides must not be in the first or the last three positions within the window. Sites meeting these criteria can be used as self-priming sites at the annealing temperature of the first PCR step.

The first PCR steps amplified the selected regions between two shuffling sites. Denaturation and annealing steps were performed at 98 °C for 2 min and 57 °C for 30 s, respectively, and primer extension was carried out at 68 °C for 30 s–2 min, repeating for 15–20 cycles. The specific combinations of primers (see Table S1 in the Supplementary Material) were used to construct the individual chimeric genes. Purified PCR products were used as template DNAs for the second overlapping PCR without primers. Finally, combined fragments were amplified in the third PCR using respective forward and reverse primers.

**Bacterial strains and plasmids.** *Escherichia coli* cultures were grown in LB medium. When appropriate ampicillin or chloramphenicol were added at a final concentration of 100 mg/l and 30 mg/l, respectively. Parental and amplified chimeric genes were cloned into the NdeI and BamHI sites of the pET21c vector system (Novagen), then transformed into *E. coli*.

**Enzyme production and purification.** Plasmids harboring a wild-type or a chimeric gene were used to transform *E. coli* BL21-CodonPlus(DE3)-RIL cells. LB ampicillin culture was inoculated and incubated at 37 °C until OD<sub>600</sub> reaches 0.6. After IPTG was added to a final concentration of 1 mM, cultures were further incubated for 4 h. Cells were harvested by centrifugation, washed and resuspended in buffer A (15 mM H<sub>3</sub>BO<sub>3</sub>, 15 mM KH-phthalate and 15 mM KH<sub>2</sub>PO<sub>4</sub>, pH 6.0).

The resuspended cells were disrupted by sonication and the homogenate was centrifuged at 8000 rpm for 10 min to remove cell debris. The lysate was heat treated at 50 °C for 30 min and centrifuged at 8000 rpm for 10 min. Proteins precipitated between 40% and 70% saturation of (NH<sub>4</sub>)<sub>2</sub>SO<sub>4</sub> were collected by centrifugation, redissolved in buffer A. Protein solutions were ultrafiltrated to remove low and high molecular weight contaminants using membranes with cut-off point 10 and 50 kDa, respectively.

**Assay of xylanase activity and protein determination.** Xylanase activity was determined by measuring the increase in reducing groups during the enzymatic hydrolysis of xylan by the dinitrosalicylic acid method of Bernfeld [19]. Standard assay mixtures (500 µl) contained 1% oat spelts xylan in buffer A, plus appropriately diluted enzyme. Incubation conditions were 10 min at appropriate temperature. The kinetic parameters  $k_{cat}$  and  $K_m$  were determined at the optimum working temperatures of the enzymes by the Eadie-Hofstee plot from three independent experiments, and at five substrate concentrations.

Protein concentration was determined by the bicinchoninic acid (BCA) method using BSA as standard as well as by UV absorbance at 280 nm. Respective theoretical molar extinction coefficient calculated by ProtParam [20] was used.

**CD spectropolarimetry and DSC.** Thermal unfolding curves and the apparent melting temperatures were determined with a differential scanning calorimeter (Microcal VP-DSC) and with a CD spectropolarimeter (Jasco J720). The heating rate was set to 2 and 1 °C/min, respectively. Prior to the measurement protein

samples were dialyzed overnight in 45 mM potassium-phosphate, pH 6.0 and diluted to 0.1–0.4 mg/ml.

**Homology modeling.** Homology models were built for TmxAcet and the chimeras BA<sub>4</sub>B, BA<sub>5</sub> and A<sub>5</sub>B using the X-ray structure of TmxB (PDB entry 1vbu) as a template. Sequence alignments were prepared with the T-Coffee program [21]. The models were built by version 9.3 of the Modeller program [22]. The automodel protocol was used with very thorough variable target function optimization followed by thorough molecular dynamics optimization. Twenty-five models were generated for each target, and the one having the lowest value of the objective function was selected as the final model.

**Estimation of effective contact energies.** Effective side chain contact energies were calculated using the Miyazawa-Jernigan contact energy matrix [23]. Contacts were defined as residue pairs with side chain centers of mass closer than 6.5 Å to each other. Effective interaction energies between two protein regions were calculated by summing up the side chain contact energies.

## Results and discussion

### Characterization of parental and chimeric enzymes

In this work, we have generated twenty-one out of the possible 62 ( $2^6 = 64$ , minus the two parental enzymes) chimeric xylanases by combining segments from a thermophilic and a hyperthermophilic xylanase variants, thereby obtaining a range of active enzymes with various temperature optima ranging from 61 to 80 °C (Fig. 1). After experimental characterization of these chimeras, we noticed the likely importance of the interaction between the N- and C-termini. Based on the activity screening measurements, the six chimeric enzymes in which the N- or C-terminal segments or both had been replaced were characterized in detail by circular dichroism (CD) and differential scanning calorimetry (DSC). These chimeric enzymes were compared with TmxAcet and TmxB with respect to their optimum working temperatures and melting temperatures (Table 1). BA<sub>4</sub>B was the most stable chimera, with a temperature optimum 12 °C higher than that of TmxAcet. The optimum temperatures of the other five chimeras were around or even less than that of TmxAcet (Fig. 2 and Fig. 3). Those chimeras (BA<sub>5</sub> and B<sub>5</sub>A) of which the thermophilic N-terminus was replaced by the respective hyperthermophilic segment(s) were inactive regardless of the length of the replaced fragment. The calorimetric curves of chimeric enzymes and thermophilic TmxAcet displayed two melting temperatures. The first melting temperature ( $T_{m1}$ , in Table 1), which is usually near the optimum working temperature, corresponds to a reversible change in tertiary structure (CD and DSC data not shown) that results in a rapid inactivation of the enzyme. The second peak corresponds to the irreversible unfolding of the overall structure. The DSC scans showed that the thermal unfolding of each enzyme is irreversible, and there was evident precipitation of the proteins. The results show that replacing only one of the two terminal segments of TmxAcet by the corresponding segment from TmxB (i.e. chimeras BA<sub>5</sub>/A<sub>5</sub>B and AB<sub>5</sub>/B<sub>5</sub>A) results in destabilization, but when both terminal segments are replaced (chimera BA<sub>4</sub>B and AB<sub>4</sub>A), a significant stabilization can be observed (see data in Table 1).

In a previous study [24], Numata et al. constructed chimeric isopropylmalate dehydrogenases by combining fragments from a thermophilic and a mesophilic variant. They found that the thermal stability of the chimeric enzymes was nearly proportional to the fraction of the sequence coming from the thermophilic variant, suggesting that the residues having a stabilizing effect distribute nearly evenly along the sequence. In contrast to these results, the stability of our chimeric xylanases is not proportional to the content of the

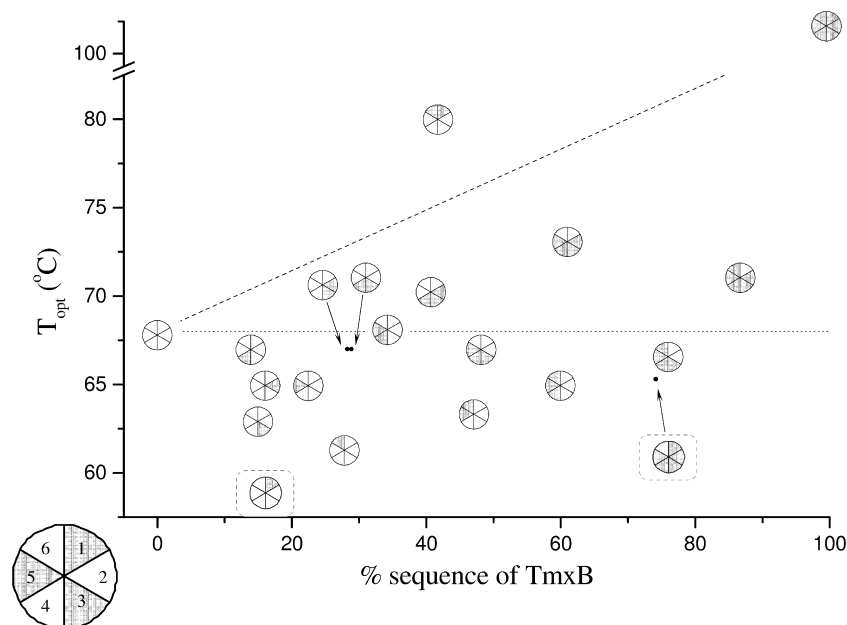


**Fig. 1.** The optimum working temperatures of chimeric xylanases as a function of the fraction of residues from the hyperthermophilic TmxB parental enzyme. Parental enzymes and chimeric constructs are represented by circles reflecting the ring-like architecture of the  $(\beta\alpha)_8$ -barrel. The circles in dotted frames represent those chimeras ( $BA_5$ ,  $B_5A$ ) that did not show any activity on xylan, therefore the first melting temperatures ( $T_{m1}$ ) of them were plotted ( $B_2A_4$ ,  $B_3A_3$ ,  $B_4A_2$  chimeras were also inactive, but these enzymes were not characterized by DSC). Plain and dotted sectors within the circles represent segments from TmxAcat and TmxB, respectively, numbered consecutively from the N- to the C-terminus as illustrated bottom left. The horizontal dotted line indicates the optimum working temperature of TmxAcat, and the dashed line represents a hypothetical linear relationship between TmxB fraction and temperature optima.

**Table 1**

Optimum working temperatures ( $T_{opt}$ ) and melting temperatures ( $T_{m1}$  and  $T_{m2}$ ) of parental and selected chimeric enzymes

Enzyme	$T_{opt}$ (°C)	( $T_{m1}$ (°C))	( $T_{m2}$ (°C))
TmxAcat	68	70.4	91.1
$BA_5$	Inactive	58.7	69.8
$A_5B$	61	63.2	78.3
$BA_4B$	80	84.1	91.0
TmxB	102	102.5	—
$B_5A$	Inactive	65.3	80.8
$AB_5$	71	72.3	85.5
$AB_4A$	73	75.5	79.6

Optimum working temperatures and melting temperatures were determined by xylanase activity assay and differential scanning calorimetry (DSC), respectively. Calorimetric measurements resulted in two-peak curves except for TmxB. The first melting temperature ( $T_{m1}$ ) corresponds to a reversible change in tertiary structure that inactivates the enzyme rapidly, whereas the second peak ( $T_{m2}$ ) corresponds to the irreversible unfolding of the overall structure.

amino acid sequence from the hyperthermophilic TmxB, and the relationship is not even monotonically increasing (see Fig. 1). As Fig. 1 shows, most chimeras (12 out of 16) have a lower temperature optimum than even the thermophilic TmxAcat enzyme. Our findings suggest that in family-10 xylanases, stabilizing residues are not evenly distributed along the sequence; rather, the terminal regions, and especially the interactions between the two termini, contribute more to the overall stability of the enzyme than the rest of the protein.

#### Kinetic parameters

Out of the six chimeras selected for detailed characterization, four had an enzymatic activity. The enzyme kinetic parameters of these constructs were determined at their optimum working temperatures. Kinetic constants for the parental and chimeric enzymes are shown in Table 2. The  $K_m$  values obtained for the chimeric enzymes are comparable to those of the parental enzymes, with

a variation below 30%. A larger variation was observed in  $k_{cat}$  values. The  $k_{cat}$  values for chimeric xylanases with terminal segments from the same parental enzyme ( $AB_4A$  and  $BA_4B$ ) are comparable to those of TmxAcat and TmxB, but for the two constructs with terminal segments from different parental enzymes ( $A_5B$  and  $AB_5$ ),  $k_{cat}$  values are about half of those of the parental enzymes. A similar statement can be made with regard to the  $k_{cat}/K_m$  values.

#### Interaction energies between the N- and C-termini

Using the available three-dimensional structure of TmxB and homology models of TmxAcat as well as the chimeras  $BA_4B$ ,  $A_5B$  and  $BA_5$ , we calculated effective interaction energies between the N-terminal 50 residues and the C-terminal segment after residue 250, roughly corresponding to segments 1 and 6 in each structure. Fig. 4 shows the negatives of the calculated energies (i.e. a higher value means stronger interaction) for each structure, and it also shows the contributions of various interaction types to the total interaction energies. For TmxB, the interaction energy between the termini is much more favorable than in TmxAcat ( $-189$  vs.  $-126$  U). It appears that this interaction is far from optimal in TmxAcat, and can be made stronger by introducing new aromatic-aromatic and aromatic-hydrophobic contacts. As expected, the total interaction energy and its composition are nearly the same in the  $BA_4B$  chimera as in TmxB. In the  $BA_5$  chimera, the total interaction energy is less favorable ( $-120$  U) than even in TmxAcat, and the relative contributions of various interaction types are similar to those of TmxAcat, with few hydrophobic-hydrophobic and hydrophobic-aromatic contacts. This indicates that the N-terminal hyperthermophilic segment and the C-terminal thermophilic segment do not match each other very well. Replacing both termini, however, results in the N-to-C interface being transferred along with the two segments, and results in a net gain in thermal stability. For the TmxAcat and TmxB molecules as well as the  $BA_4B$  and  $BA_5$  chimeras, the calculated interaction energies correlate well with the temperatures belonging to the first peaks observed in

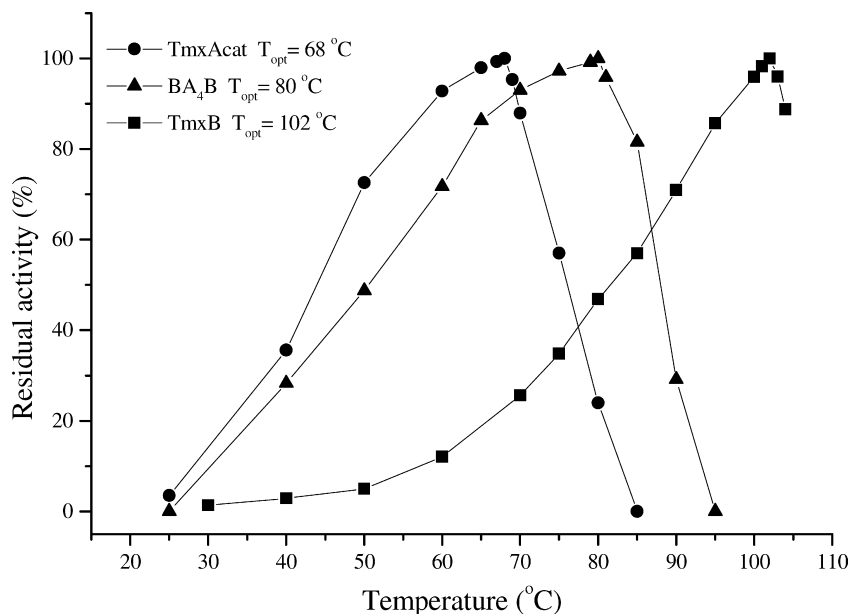


**Fig. 2.** Effect of temperature on the activity and stability of parental and chimeric xylanases. Residual activity of TmxAcat (●), BA<sub>4</sub>B chimera (▲) and TmxB (■) for the hydrolysis of xylan. The temperature profile was measured at different temperatures using the standard assay as described in the Materials and methods section at pH 6.0, in buffer A.

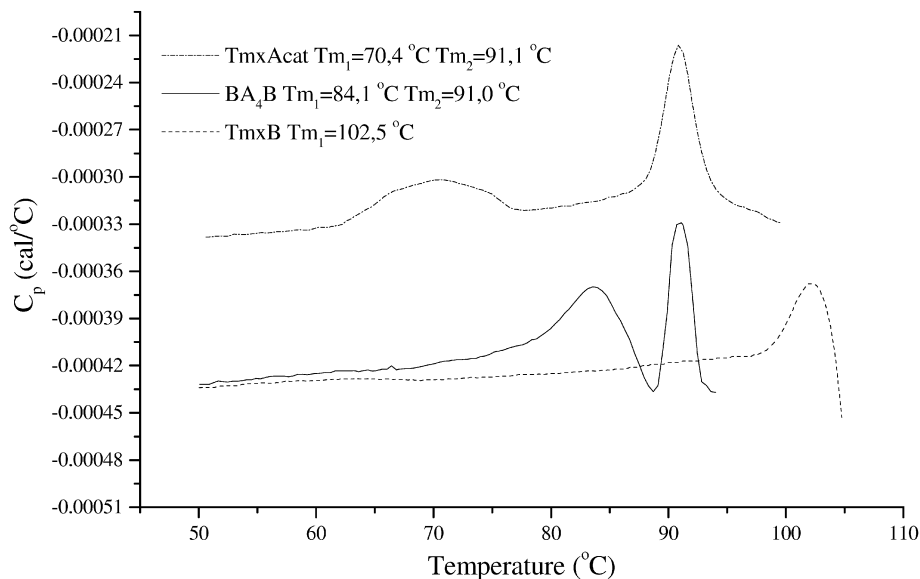


**Fig. 3.** Partial heat capacity curves of the parental enzymes and the BA<sub>4</sub>B chimeric xylanase. Partial heat capacity curves of TmxAcat (dashed-dotted line), BA<sub>4</sub>B chimera (solid line) and TmxB (dashed line). The measurements were carried out with a heating rate of 120 °C/h in 45 mM potassium-phosphate buffer, pH 6.0, the protein concentration was 0.1–0.4 mg/ml. The unfolding was irreversible.

**Table 2**

Kinetic parameters of parental and chimeric xylanases for the hydrolysis of oat speltz xylan

Enzyme	$K_m$ (mg ml <sup>-1</sup> )	$k_{cat}$ (s <sup>-1</sup> )	$k_{cat}/K_m$ (ml mg <sup>-1</sup> s <sup>-1</sup> )
TmxAcat	5.15	1024	199
TmxB	3.89	1256	323
AB <sub>4</sub> A	4.12	895	218
AB <sub>5</sub>	4.75	612	129
A <sub>5</sub> B	5.02	591	118
BA <sub>4</sub> B	4.55	1068	235

Xylanase activities were determined at the optimum working temperature of each enzyme using soluble xylan in buffer A, pH 6.0. The concentration of soluble xylan ranged from 0.2 to 20 mg/ml.

the heat capacity curves. For the A<sub>5</sub>B chimera, our calculations yield a more favorable interaction energy than expected on the basis of the measured melting temperature; however, they are in accord with the finding that A<sub>5</sub>B is more stable than BA<sub>5</sub>.

### Conclusions

The structural determinants of the stability of (β/α)<sub>8</sub>-barrel proteins have been studied extensively [25]. An analysis of ~70 structures found that most stabilizing residues contribute to the eight-stranded β-sheet [26]. A study using combinatorial mutagenesis [27] and a computational study [28] showed that the loops at the bottom of the barrel (the αβ-loops) are more important for

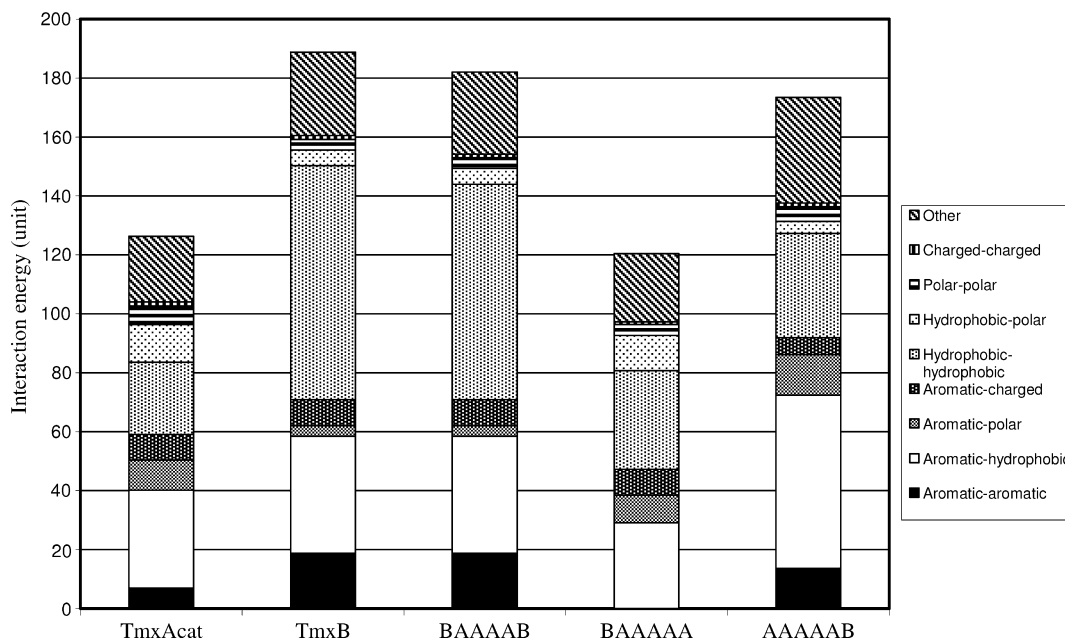


**Fig. 4.** Calculated effective interaction energies between the N- and C-termini of the parental enzymes and the BA<sub>4</sub>B, BA<sub>5</sub> and A<sub>5</sub>B chimeras. The negatives of the calculated energies are shown (i.e., a higher value means stronger interaction). Each column is divided into blocks with heights proportional to the contribution of various types of interactions (see key on the right).

stability than those at the top side ( $\beta\alpha$ -loops), suggesting a “division of labor” between the two faces of the protein. The ring-like architecture of the ( $\beta\alpha$ )<sub>8</sub>-barrel entails that the two terminal ( $\beta\alpha$ ) segments are in contact, forming similar interactions as neighboring ( $\beta\alpha$ ) units. A few studies showed that these regions may also be important for stability. In indoleglycerol phosphate synthase from *T. maritima*, the stabilizing role of a salt bridge fixing the N-terminus to the core, and that of another salt bridge serving as a clamp between helices  $\alpha_1$  and  $\alpha_8$  was demonstrated [29].

Investigations of detailed unfolding pathways of ( $\beta\alpha$ )<sub>8</sub>-barrel proteins suggested various unfolding mechanisms including the 6 + 2 and the 3 + 3 + 2 mechanisms, which both involve the disruption of the last two strands and three helices early during unfolding [30–32]. By strengthening the interactions between the terminal regions, the activation energy of this initial step can be increased, resulting in an enhanced resistance against global unfolding.

Our results suggest that combining and mixing segments from a thermophilic and a hyperthermophilic ( $\beta\alpha$ )<sub>8</sub>-barrel enzyme can be an effective and simple way to generate enzymes with an engineered optimum working temperature and structural stability. However, not all chimeric constructs had the expected higher thermal stability, which teaches us the lesson that the network of interactions between the replaced segments and their environment should be examined when selecting segments for replacement; even the introduction of a segment with a high intrinsic stability may lead to overall destabilization when its interactions with its surroundings are unfavorable. We have successfully shifted the optimum working temperature of a thermophilic xylanase into the hyperthermophilic range. The analysis of the results obtained with selected chimeric enzymes showed that the interactions between the two terminal regions have a major contribution to thermostability. The results may be generalizable to other enzymes where the N- and C-termini are in contact.

#### Acknowledgment

This work was supported by the Hungarian Scientific Research Fund (Grants OTKA 061915 and PD73096).

#### Appendix A. Supplementary data

Supplementary data associated with this article can be found, in the online version, at doi:10.1016/j.bbrc.2008.07.095.

#### References

- [1] A. Szilágyi, P. Závodszy, Structural differences between mesophilic, moderately thermophilic and extremely thermophilic protein subunits: results of a comprehensive survey, *Structure* 8 (2000) 493–504.
- [2] A. Razvi, J.M. Scholtz, Lessons in stability from thermophilic proteins, *Protein Sci.* 15 (2006) 1569–1578.
- [3] C. Vieille, G.J. Zeikus, Hyperthermophilic enzymes: sources, uses, and molecular mechanisms for thermostability, *Microbiol. Mol. Biol. Rev.* 65 (2001) 1–43.
- [4] M. Robinson-Rechavi, A. Godzik, Structural Genomics of *Thermotoga maritima* proteins shows that contact order is a major determinant of protein thermostability, *Structure* 13 (2005) 857–860.
- [5] Ihsanawati, T. Kumasaka, T. Kaneko, C. Morokuma, R. Yatsunami, T. Sato, S. Nakamura, N. Tanaka, Structural basis of the substrate subsite and the highly thermal stability of xylanase 10B from *Thermotoga maritima* MSB8, *Proteins* 61 (2005) 999–1009.
- [6] M. Robinson-Rechavi, A. Alibes, A. Godzik, Contribution of electrostatic interactions, compactness and quaternary structure to protein thermostability: lessons from structural genomics of *Thermotoga maritima*, *J. Mol. Biol.* 356 (2006) 547–557.
- [7] N. Nagano, C.A. Orengo, J.M. Thornton, One fold with many functions: the evolutionary relationships between TIM barrel families based on their sequences, structures and functions, *J. Mol. Biol.* 321 (2002) 741–765.
- [8] H. Shibuya, S. Kaneko, K. Hayashi, Enhancement of the thermostability and hydrolytic activity of xylanase by random gene shuffling, *Biochem. J.* 349 (2000) 651–656.
- [9] T. Kaper, S.J. Brouns, A.C. Geerling, W.M. De Vos, J. Van der Oost, DNA family shuffling of hyperthermostable beta-glycosidases, *Biochem. J.* 368 (2002) 461–470.
- [10] H. Xie, J. Flint, M. Vardakou, J.H. Lakey, R.J. Lewis, H.J. Gilbert, C. Dumon, Probing the structural basis for the difference in thermostability displayed by family 10 xylanases, *J. Mol. Biol.* 360 (2006) 157–167.
- [11] A. White, D. Tull, K. Johns, S.G. Withers, D.R. Rose, Crystallographic observation of a covalent catalytic intermediate in a beta-glycosidase, *Nat. Struct. Biol.* 3 (1996) 149–154.
- [12] S.J. Charnock, T.D. Spurway, H. Xie, M.H. Beylot, R. Virden, R.A. Warren, G.P. Hazlewood, H.J. Gilbert, The topology of the substrate binding clefts of glycosyl hydrolase family 10 xylanases are not conserved, *J. Biol. Chem.* 273 (1998) 32187–32199.
- [13] G.W. Harris, J.A. Jenkins, I. Connerton, N. Cummings, L. Lo Leggio, M. Scott, G.P. Hazlewood, J.I. Laurie, H.J. Gilbert, R.W. Pickersgill, Structure of the

- catalytic core of the family F xylanase from *Pseudomonas fluorescens* and identification of the xylopentaose-binding sites, *Structure* 2 (1994) 1107–1116.
- [14] A. Cramer, S.A. Raillard, E. Bermudez, W.P. Stemmer, DNA shuffling of a family of genes from diverse species accelerates directed evolution, *Nature* 391 (1998) 288–291.
- [15] C. Winterhalter, W. Liebl, Two extremely thermostable xylanases of the hyperthermophilic bacterium *Thermotoga maritima* MSB8, *Appl. Environ. Microbiol.* 61 (1995) 1810–1815.
- [16] J. Zhengqiang, A. Kobayashi, M.M. Ahsan, L. Lite, M. Kitaoka, K. Hayashi, Characterization of a thermostable family 10 endo-xylanase (XynB) from *Thermotoga maritima* that cleaves *p*-nitrophenyl-beta-D-xyloside, *J. Biosci. Bioeng.* 92 (2001) 423–428.
- [17] C. Winterhalter, P. Heinrich, A. Candussio, G. Wich, W. Liebl, Identification of a novel cellulose-binding domain within the multidomain 120 kDa xylanase XynA of the hyperthermophilic bacterium *Thermotoga maritima*, *Mol. Microbiol.* 15 (1995) 431–444.
- [18] X. Huang, W. Miller, A time-efficient, linear-space local similarity algorithm, *Adv. Appl. Math.* 12 (1991) 337–357.
- [19] P. Bernfeld, Amylases  $\alpha$  and  $\beta$ , *Methods Enzymol.* 1 (1955) 149–158.
- [20] E. Gasteiger, C. Hoogland, A. Gattiker, S. Duvaud, M.R. Wilkins, R.D. Appel, A. Bairoch, Protein identification and analysis tools on the ExPASy server, in: J.M. Walker (Ed.), *The Proteomics Protocols Handbook*, Humana Press, 2005, pp. 571–607.
- [21] C. Notredame, D.G. Higgins, J. Heringa, T-Coffee: a novel method for fast and accurate multiple sequence alignment, *J. Mol. Biol.* 302 (2000) 205–217.
- [22] A. Sali, T.L. Blundell, Comparative protein modelling by satisfaction of spatial restraints, *J. Mol. Biol.* 234 (1993) 779–815.
- [23] S. Miyazawa, R.L. Jernigan, Estimation of effective interresidue contact energies from protein crystal structures: quasi-chemical approximation, *Macromolecules* 18 (1985) 534–552.
- [24] K. Numata, M. Muro, N. Akutsu, Y. Nosoh, A. Yamagishi, T. Oshima, Thermal stability of chimeric isopropylmalate dehydrogenase genes constructed from a thermophile and a mesophile, *Prot. Eng.* 8 (1995) 39–43.
- [25] R. Sterner, B. Höcker, Catalytic versatility, stability, and evolution of the (beta/alpha)<sub>8</sub>-barrel enzyme fold, *Chem. Rev.* 105 (2005) 4038–4055.
- [26] M.M. Gromiha, G. Pujadas, C. Magyar, S. Selvaraj, I. Simon, Locating the stabilizing residues in (alpha/beta)<sub>8</sub> barrel proteins based on hydrophobicity, long-range interactions, and sequence conservation, *Proteins* 55 (2004) 316–329.
- [27] J.A. Silverman, R. Balakrishnan, P.B. Harbury, Reverse engineering the (beta/alpha)<sub>8</sub> barrel fold, *Proc. Natl. Acad. Sci. USA* 98 (2001) 3092–3097.
- [28] M. Wiederstein, M.J. Sippl, Protein sequence randomization: efficient estimation of protein stability using knowledge-based potentials, *J. Mol. Biol.* 345 (2005) 1199–1212.
- [29] A. Merz, T. Knöchel, J.N. Jansonius, K. Kirschner, The hyperthermostable indoleglycerol phosphate synthase from *Thermotoga maritima* is destabilized by mutational disruption of two solvent-exposed salt bridges, *J. Mol. Biol.* 288 (1999) 753–763.
- [30] J.M. Thornton, B.L. Sibanda, Amino and carboxy-terminal regions in globular proteins, *J. Mol. Biol.* 167 (1983) 443–460.
- [31] S. Akanuma, H. Miyagawa, K. Kitamura, A. Yamagishi, A detailed unfolding pathway of a (beta/alpha)<sub>8</sub>-barrel protein as studied by molecular dynamics simulations, *Proteins* 58 (2005) 538–546.
- [32] J.A. Silverman, P.B. Harbury, The equilibrium unfolding pathway of a (beta/alpha)<sub>8</sub> barrel, *J. Mol. Biol.* 324 (2002) 1031–1040.